CONTROL OF SLIDING-ISOLATED BUILDINGS USING SLIDING-MODE CONTROL

By J. N. Yang,[1] Fellow, ASCE, J. C. Wu,[2] A. M. Reinhorn,[3] and M. Riley[4]

ABSTRACT: Based on the theory of continuous sliding-mode control, control methods are presented for seismic-excited buildings isolated by a frictional-type sliding-isolation system. The dynamic behavior of the building equipped with a base-sliding-isolation system is highly nonlinear, and the sliding-mode–control method is ideal for such nonlinear systems. In addition to full-state-feedback controllers, a simple static-output-feedback controller using only the measured information from a few sensors installed at strategic locations without an observer is presented. The continuous sliding-mode controllers presented do not have undesirable chattering effect. Simulation results for an eight-story building indicate that (1) the control methods are robust; and (2) the control performance is outstanding. A shaking-table experimental program was conducted to verify the proposed static output control method. For the shaking-table tests, a three-story quarter-scale building model was mounted on a base mate that was supported by four frictional bearings. Experimental test results indicate that the control performance is quite remarkable, although a slight degradation was observed due to noise pollution and system time delays.

INTRODUCTION

Recently, aseismic hybrid protective systems have received considerable attention. For the hybrid protective system consisting of sliding-isolation system and actuators, the sliding isolators are used to reduce the ground motion transmitted to the building, whereas the actuators are used to reduce the response of the building, or protect the base sliding system, or both (e.g., Nagarajaiah et al. 1992, 1993; Reinhorn et al. 1993a,b). Since the dynamic behavior of base-sliding isolators is highly nonlinear, the use of such a hybrid protective system involves active control of nonlinear systems. Various control methods have been investigated for such a hybrid system including acceleration control (e.g., Nagarajaiah et al. 1992, 1993), frictional force control (e.g., Reinhorn et al. 1993a,b), instantaneous optimal control (Yang et al. 1992), dynamic linearization (e.g., Riley et al. 1993; Yang et al. 1994a), and fuzzy-set control (e.g., Reinhorn et al. 1993a,b; Riley et al. 1993). Recently, the method of sliding-mode control (SMC) or variable structure system (VSS) has been suggested by Yang et al. (1993) for this type of hybrid protective systems. While control theories for linear structures are well developed and active control systems have been installed in full-scale linear structures (e.g., Soong 1990), investigations are needed to explore promising control methods that are effective and robust for applications to control of nonlinear systems, such as the sliding-isolated buildings.

Based on the theory of VSS or SMC (e.g., Utkin 1992; Young 1993), control methods are presented in this paper for sliding-isolated buildings subjected to earthquake excitations. The theory of VSS or SMC was developed for robust control of uncertain nonlinear systems, and therefore is ideal for applications to control sliding-isolated buildings. In particular, continuous sliding-mode controllers are presented, which do not have undesirable chattering effect. For practical implementations of control systems in tall buildings, it may not be possible to install all sensors necessary to measure the full state vector because of the large number of degrees of freedom involved. On the other hand, an observer may require a significant amount of on-line computational effort, resulting in a system time delay. In this paper, static-output-feedback controllers using only the measured information from a few sensors installed at strategic locations without an observer are also presented to facilitate the practical implementations. Simulation results for a sliding-isolated eight-story building indicate that not only are the control methods robust but their performance is outstanding as well.

A shaking-table experimental test program was conducted at the National Center for Earthquake Engineering Research (NCEER), Buffalo, N.Y., to verify a static-output-feedback control method presented. The test specimen used was a three-story, quarter-scaled building model that was used extensively (e.g., Chung et al. 1989; Dyke et al. 1994; Reinhorn et al. 1993b; Yang et al. 1993, 1994c). This scaled building model was mounted on a base mate that was supported by four frictional sliding bearings. The sliding bearings were made of Teflon/stainless-steel plates. Three different earthquake records—El Centro, Hachinoke, and Pacoima—were used as the input excitations. Experimental results show slight degradations of the control performance as compared with the ideal simulation results due to noise pollutions and system time delays. Nevertheless, the control performance demonstrated by experimental results is quite satisfactory.

EQUATION OF MOTION OF STRUCTURAL SYSTEM

Consider an n-degree-of-freedom linear building structure equipped with a base-sliding-isolation system and actuators, as shown in Fig. 1. The vector equation of motion for the superstructure subjected to a one-dimensional earthquake ground motion is given by

$$\mathbf{M}\ddot{\mathbf{X}}(t) + \mathbf{C}\dot{\mathbf{X}}(t) + \mathbf{K}\mathbf{X}(t) = -\xi \ddot{y}_b(t) \tag{1}$$

in which $\mathbf{X}(t) = (x_n, x_{n-1}, \ldots, x_1)'$ = an n-vector with $x_i(t)$ being the drift of the ith story unit; $\mathbf{M}$, $\mathbf{C}$ and $\mathbf{K}$ = the (nxn) mass, damping, and stiffness matrices, respectively, for the superstructure; $\xi = (m_n, m_{n-1}, \ldots, m_1)'$ = an n-vector with m_i being the mass of ith floor; $y_b(t)$ = the absolute displacement of the base sliding system; and a prime denotes the transpose of either a vector or a matrix. The equation of motion for the base-sliding system is given by

[1]Prof., Dept. of Civ. and Envir. Engrg., Univ. of Calif., Irvine, CA 92717.
[2]Grad. Student, Dept. of Civ. and Envir. Engrg., Univ. of Calif., Irvine, CA.
[3]Prof., Dept. of Civ. Engrg., State Univ. of New York, Buffalo, NY 14260.
[4]Grad. Student, Dept. of Civ. Engrg., State Univ. of New York, Buffalo, NY.

Note. Associate Editor: Kevin Truman. Discussion open until July 1, 1996. To extend the closing date one month, a written request must be filed with the ASCE Manager of Journals. The manuscript for this paper was submitted for review and possible publication on September 14, 1994. This paper is part of the ***Journal of Structural Engineering***, Vol. 122, No. 2, February, 1996. ©ASCE, ISSN 0733-9445/96/0002-0179–0186/$4.00 + $.50 per page. Paper No. 9227.

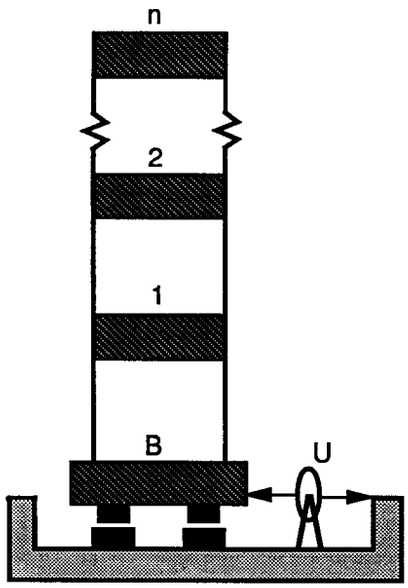

FIG. 1. Sliding-Isolated Building Model

$$\sum_{i=1}^{n} m_i \left(\ddot{y}_b + \sum_{k=1}^{i} \ddot{x}_k \right) + m_b \ddot{y}_b(t) + k_b y_b(t) + f(t) = k_b x_0 + u(t) \tag{2}$$

in which m_b = the mass of the base floor; x_0 = the ground displacement; k_b = the stiffness of the added springs to the sliding isolators as the restraining system; $f(t)$ = the frictional force from the sliding isolators; and $u(t)$ = the control force from actuators. The frictional force of the sliding bearings is given by

$$f(t) = \mu \bar{m} g \nu(t) \tag{3}$$

in which $\bar{m}g = w$ = the weight of the structural system above the sliding bearing; and μ = the coefficient of friction. In general, the coefficient of friction μ of the sliding isolator may be velocity-dependent. An approximate expression for the frictional coefficient of sliding bearings using Teflon/stainless-steel plates is obtained experimentally (e.g., Reinhorn et al. 1993b):

$$\mu = \mu_m - \mu_f e^{-a_\mu |\dot{x}_b|} \tag{4}$$

in which μ_m, μ_f, and a_μ = constants to be determined experimentally using curve-fitting procedures; and $x_b = y_b - x_0$ = the relative displacement of the sliding system. The constants μ_m, μ_f, and a_μ depend on the surface condition and the pressure of sliding bearings.

In (3), $\nu(t)$ is the hysteretic component of the sliding bearings governed by

$$\dot{\nu}(t) = D_y^{-1}(\alpha \dot{x}_b - \beta |\dot{x}_b| |\nu|^{\eta-1}\nu - \gamma \dot{x}_b |\nu|^{\eta}) \tag{5}$$

where D_y = the yield deformation; and α, β, γ, and η = the parameters defining the characteristics of the hysteresis loop of the frictional force. For $\alpha/(\beta + \gamma) = 1$, the model is identical to the viscoplastic system (Reinhorn et al. 1993b).

It should be mentioned that (1) and (2) hold for a general structure not restricted to the usual assumption of shear-beam–type buildings and that the entire structural system, including the base sliding system, has $n + 1$ degrees of freedom. The equations of motion, (1) and (2), can be cast into the state equation

$$\dot{\mathbf{Z}}(t) = \mathbf{A}\mathbf{Z}(t) - \mathbf{B}f(t) + \mathbf{B}u(t) + \mathbf{E}(t) \tag{6}$$

where $\mathbf{Z}(t)$ = a $2n + 2$ state vector; $\mathbf{A}$ = a $(2n + 2) \times (2n + 2)$ linear elastic system matrix; $\mathbf{B}$ = a $2n + 2$ vector, and $\mathbf{E}(t)$ = a $2n + 2$ excitation vector.

$$\mathbf{Z}(t) = \begin{pmatrix} \bar{\mathbf{X}}(t) \\ \dot{\bar{\mathbf{X}}}(t) \end{pmatrix} \tag{7a}$$

$$\mathbf{A} = \begin{bmatrix} \mathbf{0} & \mathbf{I} \\ -\bar{\mathbf{M}}^{-1}\bar{\mathbf{K}} & -\bar{\mathbf{M}}^{-1}\bar{\mathbf{C}} \end{bmatrix} \tag{7b}$$

$$\mathbf{E}(t) = \mathbf{B}k_b x_0(t) \tag{7c}$$

$$\bar{\mathbf{X}}(t) = (x_n, \ldots, x_1, y_b)' \tag{7d}$$

$$\mathbf{B} = \left(0, 0, \ldots, -\frac{1}{m_b}, \frac{1}{m_b}\right)' \tag{7e}$$

in which $\bar{\mathbf{M}}$, $\bar{\mathbf{C}}$ and $\bar{\mathbf{K}}$ = $(n + 1) \times (n + 1)$ mass, damping, and stiffness matrices of the entire structural system, respectively. These matrices can easily be determined from (1) and (2).

SLIDING-MODE CONTROL

Design of Sliding Surface

The first step in the sliding-mode–control method is to design the sliding surface (or switching surface) on which the response is stable. Since the coefficient matrices for both $u(t)$ and $f(t)$ are identical in (6), i.e., $\mathbf{B}$, the nonlinear frictional force $f(t)$ appears only in the equivalent control force on the sliding surface. Thus, Yang et al. (1994b) have shown that the sliding surface $S = 0$ is a linear function of the state variables, i.e.

$$S = \mathbf{P}\mathbf{Z} = 0 \tag{8}$$

in which $\mathbf{P}$ = a $2n + 2$ row vector to be determined such that the motion on the sliding surface is stable. One systematic approach for the determination of the row vector $\mathbf{P}$ is to convert the state equation of motion into the so-called regular form (e.g., Utkin 1992). Then, either the method of pole assignment or the linear-quadratic-regulator (LQR) method can be used for the determination of $\mathbf{P}$. In using the LQR method, P is determined by minimizing the integral of a quadratic function

$$J = \int_0^\infty \mathbf{Z}'(t)\mathbf{Q}\mathbf{Z}(t)\, dt \tag{9}$$

in which $\mathbf{Q}$ = a $(2n + 2) \times (2n + 2)$ positive definite matrix. Methods for determining the sliding surface or the $\mathbf{P}$ vector using either the LQR method or pole assignment are described in detail in Utkin (1992) and Yang et al. 1994b).

Design of Controller Using Lyapunov Direct Method

The next step in sliding-mode control is to construct the controller to drive the state trajectory into the sliding surface. To achieve this goal, we consider a Lyapunov function

$$V = 0.5SS \tag{10}$$

The sufficient condition for the sliding mode to occur is given by $\dot{V} = S\dot{S} \leq 0$. Substituting $S = \mathbf{P}\mathbf{Z}$ into (10), taking the derivative and using the state equation of motion, (6), one obtains

$$\dot{V} = \lambda(u - G) \tag{11}$$

in which λ and G = scalers, defined by

$$\lambda = \mathbf{S}\mathbf{P}\mathbf{B}; \quad G = -(\mathbf{P}\mathbf{B})^{-1}\mathbf{P}(\mathbf{A}\mathbf{Z} - \mathbf{B}f + \mathbf{E}) \tag{12}$$

For $\dot{V} \leq 0$, a possible continuous sliding mode controller is given by Zhou and Fisher (1992):

$$u(t) = G - \delta\lambda \tag{13}$$

in which $\delta \geq 0$ is the sliding margin. Substitution of (13) into (11) leads to $\dot{V} = -\delta\lambda^2 \leq 0$.

To examine the sliding mode controller, we substitute $u(t)$ in (13) into the state equation of motion, (6), and perform detailed manipulations using (7*a*)–(7*e*). The resulting closed-loop system is obtained as follows

$$\dot{\mathbf{Z}}(t) = [\mathbf{A} - \mathbf{B}(\mathbf{PB})^{-1}\mathbf{PA} - \delta\mathbf{BB}'\mathbf{P}'\mathbf{P}]\mathbf{Z}(t) \tag{14}$$

As (14) shows, the earthquake excitation has been completely compensated and hence the response state vector is zero. As a result, the controller in (13) completely compensates the structural response in the theoretical sense. In reality, however, a complete compensation of the response is not possible due to possible system time delays, such as the sampling rate in measuring the response quantities. Simulation results in this regard will be presented later.

Rather than a complete compensation for the response, it may be desirable to leave some restoring forces in the bearings for restraining purposes. In ths connection, the following controller with a partial compensation can be used

$$u(t) = \alpha^* G - \delta\lambda \tag{15}$$

in which $0 \leq \alpha^* \leq 1$. The stability of such a controller has been shown in Yang et al. (1994b).

STATIC OUTPUT FEEDBACK

The controller presented in the previous section requires a full-state feedback either through measurements or from an observer. For practical implementations of control systems in tall buildings, it may not be possible to install all sensors to measure the full state vector, because of the many degrees of freedom involved. On the other hand, an observer may require a significant amount of on-line computational efforts resulting in a system time delay. From the practical implementation standpoint, it is highly desirable to establish static-output-feedback controllers using only the information measured from a limited number of sensors installed at strategic locations without an observer. A static-output-feedback controller was presented by Yang et al. (1994b) for control of a general nonlinear structure as follows.

Let $\bar{\mathbf{Z}}_m$ be a $(2n + 2)$–dimensional modified observation (output) state vector consisting of m measured (output) state variables and zero elements for those state variables that are not measured, i.e., $\bar{\mathbf{Z}}_m$ is obtained from $\mathbf{Z}$ by setting state variables that are not measured to zero. Then, a stable static-output controller is given by Yang et al. (1994b).

$$u(t) = \bar{G} - \delta\lambda \tag{16}$$

in which

$$\lambda = \bar{\mathbf{Z}}_m'\mathbf{P}'\mathbf{PB}; \quad \bar{G} = -(\mathbf{PB})^{-1}\mathbf{P}(\mathbf{A}\bar{\mathbf{Z}}_m - \mathbf{B}f + \mathbf{E}) \tag{17}$$

Simple Static-Output-Feedback Controller

To estimate the frictional force developed in the sliding bearings, both the displacement $x_b = y_b - x_0$ and the velocity $\dot{x}_b = \dot{y}_b - \dot{x}_0$ of the sliding bearings should be measured. A simple static-output-feedback controller using only the available information of y_b, $\dot{y}_b$, x_0, and $\dot{x}_0$ is obtained as follows. In this case, the sliding surface becomes

$$S = p_1 y_b + \dot{y}_b \tag{18}$$

in which p_1 is a positive number to guarantee the stability of the sliding surface. Then, the sliding surface $\mathbf{P}$ and the modified observation state vector $\bar{\mathbf{Z}}_m$ are given by

$$\mathbf{P} = (0, 0, \ldots, p_1, 0, 0, \ldots, 1);$$

$$\bar{\mathbf{Z}}_m = (0, 0, \ldots, y_b, 0, 0, \ldots, \dot{y}_b)' \tag{19}$$

Substituting (18) and (19) into (16) and (17), one obtains a simple output controller

$$u(t) = \bar{G} - \delta\lambda \tag{20}$$

in which

$$\lambda = \frac{p_1 y_b + \dot{y}_b}{m_b} \tag{21a}$$

$$\bar{G} = -m_b p_1 \dot{y}_b + k_b(y_b - x_0) + \mu\bar{m}gv \tag{21b}$$

The simple output controller given by (20) and (21) is very plausible for practical implementations, since only y_b, $\dot{y}_b$, x_0, and $\dot{x}_0$ should be measured.

A careful examination for both static-output controllers presented in (16)–(21) indicate that the response of the closed-loop system is zero, since the earthquake excitation is also completely compensated. Again, due to possible system time delays, the performance of the simple static output controller in (20)–(21) will be demonstrated by simulation results later.

In the shaking-table test, however, it is necessary to limit the sliding displacement using the restraining system for safety considerations. As a result, instead of completely compensating the stiffness k_b of the restraining system, a partial cancellation is made, and (20) and (21) are modified as

$$u(t) = G^* - \delta\lambda \tag{22}$$

in which

$$\lambda = \frac{p_1 y_b + \dot{y}_b}{m_b} \tag{23a}$$

$$G^* = -m_b p_1 \dot{y}_b + \phi k_b(y_b - x_0) + \mu\bar{m}gv \tag{23b}$$

where $0 \leq \phi \leq 1$. The controller given by (22) and (23) can easily be shown to be stable by substituting it into the equations of motion, (1) and (2). This simple static output controller will be used in the experiment program. As Eq. (23) shows, the restraining system is completely compensated for $\phi = 1.0$. For $0 \leq \phi < 1$, the control performance will degrade due to the existence of the restraining system, as will be demonstrated in the experimental results later.

NUMERICAL SIMULATION

To demonstrate the applications of the sliding-mode–control methods presented here, an eight-story shear-beam–type building equipped with sliding isolators, as shown in Fig. 1, is considered. The properties of the structure are as follows: (1) The mass of each floor is identical with $m_i = m = 345.6$ t; (2) the elastic stiffnesses of the eight-story units are $k_i (i = 1, 2, \ldots, 8) = 3.4 \times 10^5$, 3.26×10^5, 2.85×10^5, 2.69×10^5, 2.43×10^5, 2.07×10^5, 1.69×10^5, and 1.37×10^5 kN/m; and (3) the viscous damping coefficients for each story unit are $c_i = 490$, 467, 410, 386, 349, 298, 243, and 196 kN·s/m. The damping coefficients result in a damping ratio of 0.38% for the first vibrational mode with the fundamental frequency of 5.24 rad/s.

For this shear-beam–type building (superstructure), elements of matrices $\mathbf{M}$, $\mathbf{C}$, and $\mathbf{K}$, [(1)] are given as follows: (1) $M(i, j) = m_{n-i+1}$ for $i = 1, 2, \ldots, n$ and $j = i, i + 1, \ldots, n$, and $M(i, j) = 0$ for $j < i$; (2) $C(i, j) = 0$ except $C(i, i) = c_{n-i+1}$ for $i = 1, 2, \ldots, n$ and $C(i, i - 1) = -c_{n-i+2}$ for $i = 2, 3, \ldots, n$; and (3) $K(i, j) = 0$ except $K(i, i) = k_{n-i+1}$, for $i = 1, 2, \ldots, n$ and $K(i, i - 1) = -k_{n-i+2}$ for $i = 2, 3, \ldots, n$.

A Teflon/stainless-steel sliding-isolation system is imple-

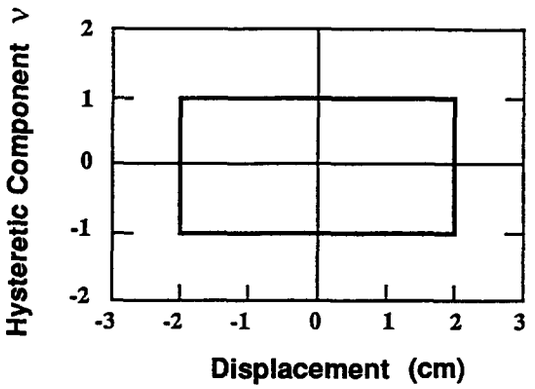

FIG. 2. Hysteresis Loop of Base-Sliding-Isolation System

mented to the building. The mass of the sliding system is m_b = 450 t, and the variable coefficient of friction μ is given by (4) with μ_m = 10%, μ_f = 5%, and a_μ = 0.2 s/cm. These parametric values are very close to experimentally determined values for Teflon/stainless-steel bearings recently obtained. The parameter values for the hysteretic behavior, (5), are α = 1.0, β = 0.5, η = 2, γ = 0.5, and D_y = 0.012 cm. No spring is added to the base-isolation system, i.e., k_b = 0. The hysteresis loop of such a sliding isolation system is shown in Fig. 2 in which the hysteretic component v is plotted as a function of the sliding displacement x_b [(5)]. With the base sliding system, the entire building has nine degrees of freedom. With the preceding information, matrices $\bar{\mathbf{M}}$, $\bar{\mathbf{C}}$, and $\bar{\mathbf{K}}$ for the entire system, (7), can be established appropriately.

The El Centro earthquake scaled to a peak ground acceleration of 0.3g is used as the input excitation. Within 30 s of the earthquake episode, the maximum interstory drifts x_i and the maximum (absolute) floor accelerations $\ddot{x}_{ai}$ of the superstructure are shown for stories 1–8 in columns 2–3 of Table 1. In Table 1, the results shown for story B represent the maximum relative displacement and the maximum absolute acceleration of the base sliding system.

To reduce the response of the building, actuators are installed in the base-isolation system as shown in Fig. 1. The LQR method, (9), is used to determine the sliding surface with a diagonal weighting matrix $\mathbf{Q}$; Q_{99} = 10, Q_{ii} = 1,000 for i = 1, 2, . . . , 8 and Q_{ii} = 0.1 for i = 10, . . . , 18. Q_{ii} for i = 1, 2, . . . , 8 correspond to the interstory drifts of the superstructure and thus are penalized heavily. On the other hand, Q_{ii} for i = 10, . . . , 18 correspond to structural velocities, which are not penalized. The continuous controller given by (13) with the sliding margin δ = 1 kN·kg·m/s is used. As shown in (14), the controller in (13) completely compensates the response, so the state vector $\mathbf{Z}(t)$ is theoretically zero. In practical applications, however, the feedback response and the ground excitation are measured at a certain sampling rate, say ω Hz, such that the control force has a time delay of $\Delta\tau = 1/\omega$ s. Based on a reasonable sampling rate of 250 Hz, i.e., a time delay of 4×10^{-3} s, the peak-response quantities and the required peak control force, U, are shown in columns 4 and 5 of Table 1, designated as FSF(I) for full state feedback. The building response quantities are quite small. The maximum control force U in Table 1 is expressed in terms of the percentage of the total weight of the structural system.

The control performance depends on the design of the sliding surface and the sliding margin. Another sliding surface determined by the LQR method with a diagonal weighting matrix $\mathbf{Q}$ is considered. The diagonal elements are as follows: Q_{99} = 50, $Q_{ii} = 10^4$ for i = 1, 2, . . . , 8 and Q_{jj} = 0.1 for j = 10, 11, . . . , 18. With the same sampling rate and the sliding margin of δ = 1 kN·kg·m/s as well as the controller in (13), the peak-response quantities of the entire building system and the required peak-control force U are shown in columns 6 and 7 of Table 1, designated as FSF(II). The control performance with such a sliding surface improves over the previous case,

TABLE 1. Maximum Response Quantities of Eight-Story Building Equipped with Hybrid Sliding Bearings: 250-Hz Sampling Rate

	(*a*) μ_m = 0.1, μ_f = 0.05, AND a_μ = 0.2									
	No Control		FSF(I), U = 10.2%		FSF(II), U = 10.2%		OF(I), U = 10.5%		OF(II), U = 10.1%	
Story (1)	x_i (cm) (2)	$\ddot{x}_{ai}$ (cm/s^2) (3)	x_i (cm) (4)	$\ddot{x}_{ai}$ (cm/s^2) (5)	x_i (cm) (6)	$\ddot{x}_{ai}$ (cm/s^2) (7)	x_i (cm) (8)	$\ddot{x}_{ai}$ (cm/s^2) (9)	x_i (cm) (10)	$\ddot{x}_{ai}$ (cm/s^2) (11)
B	9.26	395	9.94	296	9.90	255	10.20	297	9.58	295
1	1.12	327	0.03	12	0.02	6	0.06	50	0.08	47
2	1.20	425	0.02	7	0.01	3	0.07	47	0.08	58
3	1.34	409	0.02	6	0.01	3	0.08	42	0.08	53
4	1.35	482	0.02	6	0.01	3	0.10	43	0.11	53
5	1.53	369	0.02	5	0.01	3	0.07	43	0.10	46
6	1.74	465	0.02	6	0.01	3	0.11	42	0.10	56
7	1.80	417	0.02	5	0.01	3	0.12	43	0.12	46
8	1.38	474	0.02	7	0.01	5	0.13	52	0.18	70
	(*b*) μ_m = 0.1, μ_f = 0.05, AND a_μ = 0.5									
	No Control		FSF(I), U = 11.3%		FSF(II), U = 11.4%		OF(I), U = 10.5%		OF(II), U = 10.1%	
Story (12)	x_i (cm) (13)	$\ddot{x}_{ai}$ (cm/s^2) (14)	x_i (cm) (15)	$\ddot{x}_{ai}$ (cm/s^2) (16)	x_i (cm) (17)	$\ddot{x}_{ai}$ (cm/s^2) (18)	x_i (cm) (19)	$\ddot{x}_{ai}$ (cm/s^2) (20)	x_i (cm) (21)	$\ddot{x}_{ai}$ (cm/s^2) (22)
B	9.01	419	9.94	353	9.90	406	10.20	357	9.58	355
1	1.21	323	0.03	14	0.02	6	0.07	56	0.10	53
2	1.29	427	0.02	8	0.01	3	0.07	55	0.10	69
3	1.47	425	0.02	6	0.01	3	0.08	49	0.10	66
4	1.51	534	0.02	6	0.01	3	0.11	50	0.12	60
5	1.71	388	0.02	5	0.01	3	0.08	50	0.12	55
6	2.02	486	0.02	7	0.01	3	0.11	50	0.12	68
7	2.10	418	0.02	5	0.01	3	0.12	47	0.16	50
8	1.43	491	0.02	7	0.01	5	0.14	56	0.21	84

since the response quantities are further reduced. Comparisons of columns 2, 3, 6, and 7 indicate that structural response is reduced by one order of magnitude and the sliding displacement remains about the same.

We next consider the simple static output controller in (20)–(21) in which only the absolute response quantities of the base sliding system are measured, i.e., y_b and $\dot{y}_b$, in addition to the earthquake ground motion, x_0 and $\dot{x}_0$. The sliding surface is given by (18) with $p_1 = 10$ per centimeter and $\delta = 1$ kN·kg·m/s in (20) is used. Again, the simple static output controller results in a complete compensation of the building response in a theoretical sense. With a sampling rate of 250 Hz, the peak-response quantities of the entire structural system in 30 s of the earthquake episode are presented in columns 8 and 9 of Table 1, designated as OF(I) for output feedback. Another design of the sliding surface in which $p_1 = 1.0$ per centimeter and $\delta = 1$ kN·kg·m/s is considered. With the same sampling rate, the corresponding peak-response quantities are shown in columns 10 and 11 of Table 1, designated as OF(II). When p_1 is larger (i.e., $p_1 = 10$ per centimeter), the pole of the sliding surface is shifted more to the left-hand side in the complex plane; however, the performance in reducing the interstory drifts and floor acceleration is not necessarily better.

The simulation results presented in columns 2–11 of Table 1 clearly demonstrate that with a reasonable sampling rate of 250 Hz (1) the performance of the continuous sliding-mode–control method is outstanding; and (2) the performance for the static-output-feedback controller, using only the measurements of the motion of the sliding-isolation system, compares favorably with that of the full state feedback.

It should be mentioned that the sliding-isolated building considered with $\mu_m = 0.1$, $\mu_f = 0.05$, and $a_\mu = 0.2$ s/cm is identical to that considered in Yang et al. (1994a). Unfortunately there was a typographical error in Yang et al. (1994a) in which a_μ was misprinted as 0.5 s/cm. Suppose the characteristics of the frictional coefficient in (4) for the isolation system are as follows: $\mu_m = 0.1$, $\mu_f = 0.05$, and $a_\mu = 0.5$ s/cm. The same designs for the controller and the sliding surface for different cases presented in columns 2–11 of Table 1 are used. The corresponding simulation results for the peak response quantities of the building are presented in columns 13–22 of Table 1. As observed, the performances of the control designs for the upper and lower parts of Table 1 are almost identical.

As mentioned previously, the theory of variable structure system or sliding-mode control was developed for robust control of uncertain nonlinear systems. The static-output-feedback controller presented in (20) and (21) is independent of the properties of the building. Therefore, the simulation results presented in columns 8–11 of Table 1 are theoretically robust with respect to parametric uncertainties of the building. To examine the robustness of the full-state-feedback controller, we vary the stiffness of all story unit of the building by ±30%. In other words, estimation errors of ±30% for the stiffness matrix **K** of the superstructure, (1), are used to design the sliding surface and the controller. The simulation results corresponding to the same design shown in columns 6 and 7 of Table 1 are presented in Table 2. Columns 2 and 3 of Table 2, corresponding to 0% uncertainty, are identical to columns 6 and 7 of Table 1. Table 2 demonstrates that the full-state-feedback controller is robust.

TABLE 2. Robustness for Maximum Response Quantities of Eight-Story Building Equipped with Hybrid Sliding Bearings: 250-Hz Sampling Rate

	FSF(II), k + 0%, U = 10.2%		FSF(II), k − 30%, U = 10.2%		FSF(II), k + 30%, U = 10.3%	
Story (1)	x_i (cm) (2)	$\ddot{x}_{ai}$ (cm/s^2) (3)	x_i (cm) (4)	$\ddot{x}_{ai}$ (cm/s^2) (5)	x_i (cm) (6)	$\ddot{x}_{ai}$ (cm/s^2) (7)
B	9.90	255	9.90	255	9.90	255
1	0.02	6	0.02	6	0.02	5
2	0.01	3	0.01	3	0.01	3
3	0.01	3	0.01	3	0.01	3
4	0.01	3	0.01	3	0.01	3
5	0.01	3	0.01	3	0.01	3
6	0.01	3	0.01	3	0.01	3
7	0.01	3	0.01	3	0.01	3
8	0.01	5	0.01	5	0.01	4

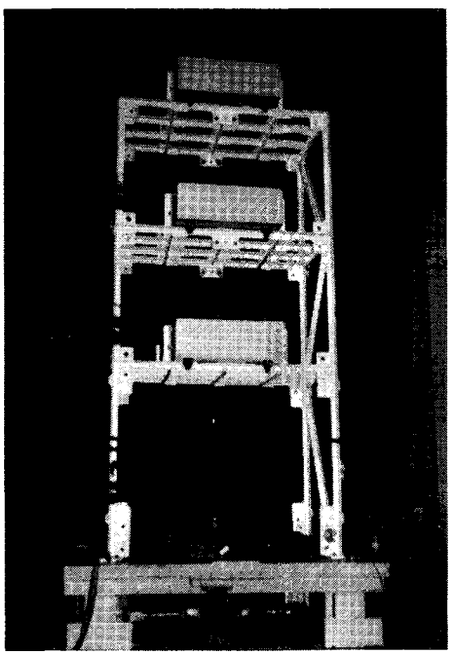

FIG. 3. A Four-Degree-of-Freedom Scaled Model Equipped with Hybrid Control System

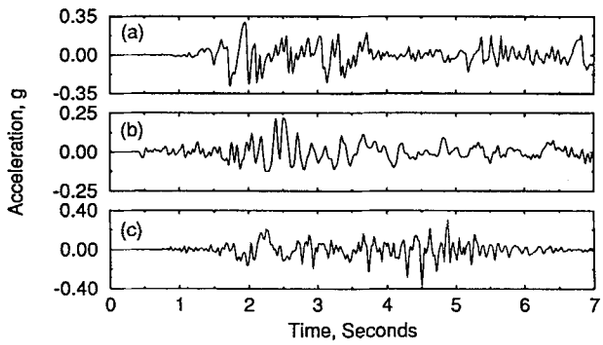

FIG. 4. Earthquake Excitations: (a) 0.34*g* El Centro Earthquake; (b) 0.23*g* Hachinohe Earthquake; (c) 0.40*g* Pacoima Earthquake

EXPERIMENTAL RESULTS

Shaking-table tests were conducted at NCEER. The same three-story quarter-scale building model described by Soong (1990) was mounted on a base mat that was supported by four sliding bearings made of Teflon/stainless-steel plates as shown in Fig. 3. Therefore, the entire structural model is a four-degree-of-freedom system. All the experimental setup, instrumentation, system identifications, and so on were reported by Reinhorn et al. (1993b). A hydraulic actuator was installed on the shaking table to control the sliding bearings (see Fig. 3). Three different earthquake records, in which the frequency is scaled by 200% and the peak ground acceleration is scaled to the appropriate magnitude, were used as the input excitations.

TABLE 3. Experimental Results for Maximum Response Quantities of Four-Degree-of-Freedom Sliding Isolated Building Model

Cases (1)	El Centro		Hachinohe		Pacoima	
	Passive (2)	Hybrid (3)	Passive (4)	Hybrid (5)	Passive (6)	Hybrid (7)
x_b (mm)	21.386	34.850	24.003	45.212	19.329	33.909
x_1 (mm)	5.330	3.023 (43%)	4.699	2.819 (40%)	4.191	2.642 (37%)
x_2 (mm)	5.537	2.743 (50%)	5.563	3.251 (42%)	4.775	2.896 (39%)
x_3 (mm)	4.674	2.489 (47%)	4.089	2.540 (38%)	3.962	2.337 (41%)
$\ddot{x}_{ab}$ (mm/s^2)	7.671	5.182 (32%)	6.629	3.734 (44%)	6.121	4.877 (20%)
$\ddot{x}_{a1}$ (mm/s^2)	6.629	6.198 (7%)	6.198	4.877 (21%)	8.204	6.172 (25%)
$\ddot{x}_{a2}$ (mm/s^2)	7.620	5.639 (26%)	7.595	4.724 (38%)	6.553	6.604 (−1%)
$\ddot{x}_{a3}$ (mm/s^2)	11.481	5.944 (48%)	8.077	5.461 (33%)	1.163	5.969 (16%)
U (%)	—	12.4	—	14.2	—	13.9

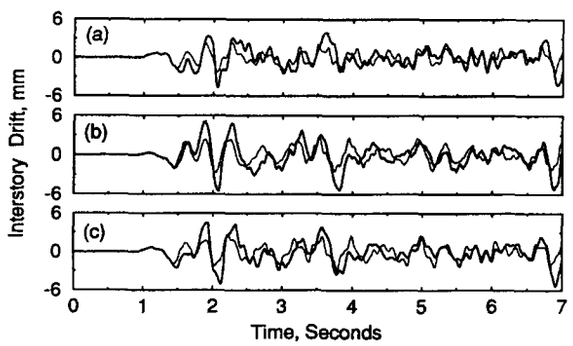

FIG. 5. Interstory Drifts of Building with Passive Control (Solid Curve) and Hybrid Control (Dotted Curve) under El Centro Earthquake; (a) Top-Story Unit; (b) Second-Story Unit; (c) First-Story Unit

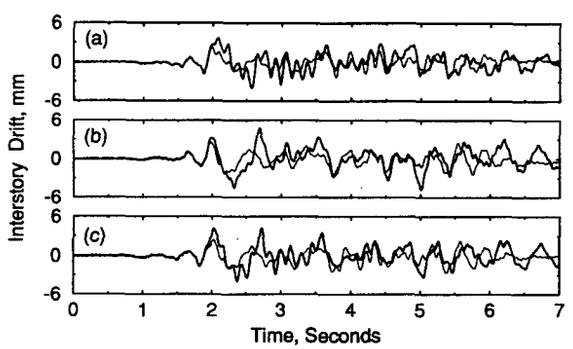

FIG. 6. Interstory Drifts of Building with Passive Control (Solid Curve) and Hybrid Control (Dotted Curve) under Pacoima Earthquake; (a) Top-Story Unit; (b) Second-Story Unit; (c) First-Story Unit

These are 0.34g El Centro earthquake, 0.23g Hachinohe earthquake, and 0.4g Pacoima earthquake, as shown in Fig. 4.

The mass of each story unit is given as follows: m_b = 1,148.62 kg (6.5544 lb·sec^2/in.) (base mat), m_i = 958 kg (5.4667 lb·sec^2/in.) for i = 1, 2, 3. Two elastic springs were added to the sliding system as the restrainers and the total elastic stiffness is k_b = 71,616.36 N/m (408.85 lb/in.) [(2)]. These elastic springs are added for precaution to prevent the test specimen from unexpected large slidings out of the bearings. The parameter values for the sliding bearings were obtained through the system identification as follows: α = 1.0, γ = β = 0.5, η = 3, D_y = 0.0254 mm (0.001 in.), μ_m = 0.06, μ_f = 0.03, and a_μ = 0.09016 s/mm (2.29 sec/in.) [(4) and (5)].

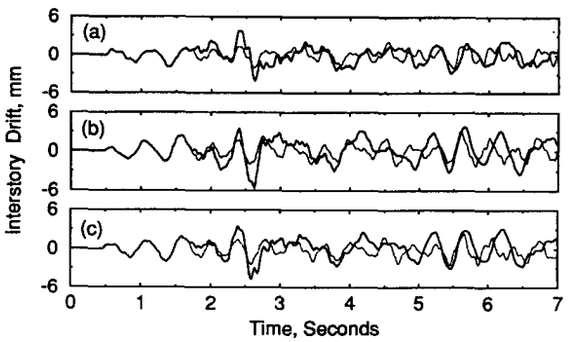

FIG. 7. Interstory Drifts of Building with Passive Control (Solid Curve) and Hybrid Control (Dotted Curve) under Hachinohe Earthquake; (a) Top-Story Unit; (b) Second-Story Unit; (c) First-Story Unit

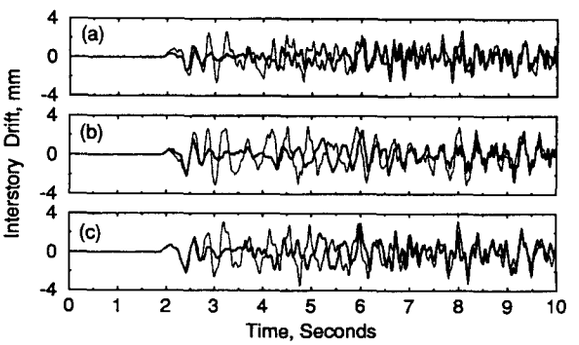

FIG. 8. Comparison of Experimental Time Histories (Dotted Curve) and Simulation Results (Solid Curve) for Interstory Drifts under El Centro Earthquake; (a) Top-Story Unit; (b) Second-Story Unit; (c) First-Story Unit

The properties of the superstructures are also obtained through system identification given by Reinhorn et al. (1993b).

To avoid heavy noise pollution and system time delays in the control operations, and to demonstrate the practical implementations of the proposed control algorithm, the simple static-output-feedback controller presented in (22) and (23) was used. Only the displacement y_b and velocity $\dot{y}_b$ of the sliding system as well as the shaking-table velocity $\dot{x}_0$ and displacement x_0, were measured and used for the control algorithm. The sliding surface is given by (18) with p_1 = 0.315 per millimeter (8.0 per inch) > 0. ϕ = 0.8 and δ = 0 were used in the controller [(22) and (23)].

Within 30 s of the earthquake episode, the peak interstory drifts of the structure $x_i (i = b, 1, 2, 3)$, the absolute accelerations of each floor $\ddot{x}_{ai} (i = b, 1, 2, 3)$, and the peak control force U are summarized in Table 3 for three different earthquake excitations. In Table 3, the peak-response quantities for the system (with sliding bearings) without actuator are designated as "passive", whereas those for the system with active control are designated as "hybrid." U is expressed as the percentage of the total system weight. Also shown in parentheses under "hybrid" are the percentages of reduction for the peak-response quantities relative to passive responses. Table 3 shows that the reduction of the maximum interstory drifts ranges from 37% to 50% whereas the reduction for the maximum floor accelerations is much less. Time histories of the interstory drifts for the three-story units of the building model are displayed in Figs. 5–7. In each figure, the solid curve represents the response of the passive system (without actuator), whereas the dotted curve denotes the response with hybrid control (actuator).

For every test series conducted, numerical simulations of the response quantities under ideal control environments were

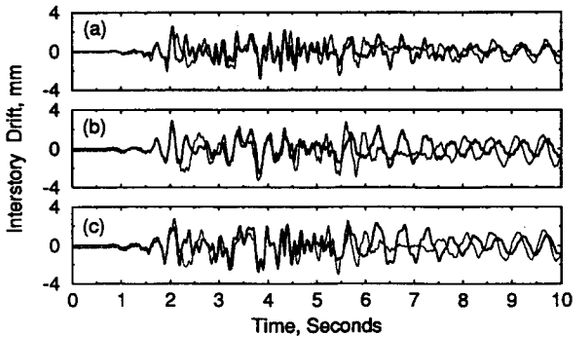

FIG. 9. Comparison of Experimental Time Histories (Dotted Curve) and Simulation Results (Solid Curve) for Interstory Drifts under Pacoima Earthquake; (a) Top-Story Unit; (b) Second-Story Unit; (c) First-Story Unit

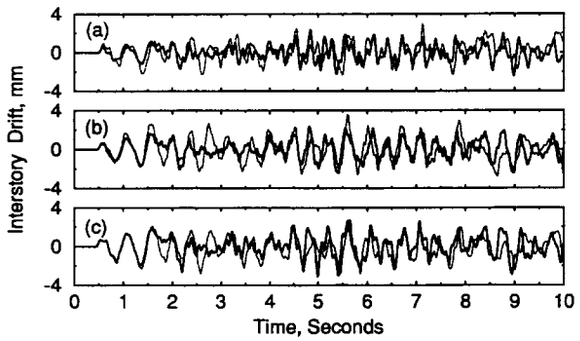

FIG. 10. Comparison of Experimental Time Histories (Dotted Curve) and Simulation Results (Solid Curve) for Interstory Drifts under Hachinohe Earthquake; (a) Top-Story Unit; (b) Second-Story Unit; (c) First-Story Unit

TABLE 4. Comparison of Maximum Response Quantities of Four-Degree-of-Freedom Sliding-Isolated Building Model between Experimental Records and Simulation Results

	El Centro		Hachinohe		Pacoima	
Cases (1)	Experiment (2)	Simulation (3)	Experiment (4)	Simulation (5)	Experiment (6)	Simulation (7)
x_b (mm)	34.849	29.083	45.212	39.345	33.909	33.376
x_1 (mm)	3.023	2.616	2.819	2.692	2.642	2.311
x_2 (mm)	2.743	2.362	3.251	2.159	2.896	2.464
x_3 (mm)	2.489	2.388	2.540	2.134	2.337	2.464
$\ddot{x}_{ab}$ (mm/s^2)	5.182	8.255	3.734	6.655	4.877	8.077
$\ddot{x}_{a1}$ (mm/s^2)	6.198	6.096	4.877	5.359	6.172	6.071
$\ddot{x}_{a2}$ (mm/s^2)	5.639	6.071	4.724	4.674	6.604	4.902
$\ddot{x}_{a3}$ (mm/s^2)	5.944	6.096	5.461	4.775	5.969	5.791
U (%)	12.4	10.4	14.2	11.9	13.9	12.0

performed. Time histories of the interstory drifts based on numerical simulations are presented as solid curves in Figs. 8–10 for different earthquake excitations. Also shown in these figures as dotted curves are the experimental records for comparison. The peak response quantities for the simulation results and the experimental data are summarized in Table 4 for comparison.

Because actuator dynamics, actuator-structure interaction and system time delay are not accounted for in the simulation, the differences between the experimental data and the simulation results are expected. In particular, the response of the building is quite sensitive to the system time delay, due to the fact that the motion of the sliding system switches from the sticking phase to the sliding phase and vice versa quite frequently. Consequently, experimental tests for control of sliding-isolated structures require elaborate efforts. Table 4 shows that the correlations for the peak-response quantities are quite satisfactory. The control performance for the simulation results is slightly better than that of the experimental data as expected. Figs. 8–10 show that the correlations for the time histories of the response quantities are also quite reasonable, except for the case of El Centro earthquake excitation, Fig. 8, where the deviation is more prominent. Based on the experimental results obtained here, the simple static-output-feedback controller presented is quite promising for control of sliding-isolated buildings under seismic excitations.

CONCLUSIONS

Based on the theory of continuous sliding-mode control or variable structure system, control methods have been presented for applications to seismic-excited buildings isolated by frictional-type sliding bearings. The continuous sliding-mode controllers presented do not have possible chattering effects. In addition to full-state-feedback controllers, static-output-feedback controllers using only the measured information from a few sensors are also presented. These static output feedback controllers can be implemented readily in practical applications. Simulation results for an eight-story sliding-isolated building demonstrate that (1) the control methods presented are robust with respect to parametric uncertainties of the building; and (2) the performance of the simple static output feedback controller is comparable to that of the full-state-feedback controller.

A shaking-table experimental program, using a three-story quarter-scale building model, has been conducted to verify the simple static-output-feedback controller presented. Such a controller can be used for practical implementation of the hybrid control systems on full-scale buildings. The correlations for the peak-response quantities between the simulation results and experimental data are quite reasonable. The correlations for the response time histories can be improved by taking into account the actuator dynamics and actuator-structure interactions in the numerical simulations, and by using better sensing devices and instrumentations in the experiments. In addition, the performance of the control methods presented can be improved if the actuator dynamics and actuator-structure interaction are taken into account in the design of the sliding surface and controllers.

ACKNOWLEDGMENTS

The research was supported by the National Science Foundation through grants BCS-91-20128 and the National Center for Earthquake Engineering Research, NCEER-93-5123.

APPENDIX. REFERENCES

Chung, L. L., Lin, R. C., Soong, T. T., and Reinhorn, A. M. (1989). "Experiments on active control for MDOF seismic structures." *J. Engrg. Mech.*, ASCE, 155(8), 1609–1627.

Dyke, S. J., Spencer, B. F., Quast, P., Saiin, M. K., and Kaspari, D. C. (1994). "Experimental verification of acceleration feedback control strategies for MDOF structures," presented at the Second International Conference on Computational Stochastic Mechanics, Athens, Greece, Jun. 13–15.

Nagarajaiah, S. M., Riley, M. A., Reinhorn, A. M., and Shinozuka, M. (1992). "Hybrid control of sliding isolated bridges." *Proc. 1992 ASME Pressure Vessels and Piping Conf.*, Am. Soc. of Mech. Engrs., New York, N.Y., 2, 83–89.

Nagarajaiah, S., Riley, M. A., and Reinhorn, A. M. (1993). "Hybrid control of sliding isolated bridges." *J. Engrg. Mech.*, ASCE, 119(11), 2317–2332.

Reinhorn, A. M., Nagarajaiah, S., Riley, M. A., and Subramanian, R. (1993a). "Hybrid control of sliding isolated structures." *Structural engineering in national hazards mitigation*, ASCE, New York, N.Y., 1, 766–771.

Reinhorn, A. M., Nagarajaiah, S., Riley, M. A., and Subramanian, R. (1993b). "Study of hybrid systems for structural and nonstructural systems." *Proc. Int. Workshop on Structural Control*, G. W. Housner and S. F. Masri, eds., 405–416.

Riley, M. A., Subramaniam, R., Nagarajaiah, S., and Reinhorn, A. M. (1993). "Hybrid control of sliding base-isolated structures." *Proc. ATC-17-1 Seminar on Seismic Isolation, Passive Energy Dissipation and Active Control*, Appl. Technol. Council, 799–810.

Soong, T. T. (1990). *Active structural control: Theory and practice*. Longman Scientific and Technical, New York, N.Y.

Utkin, V. I. (1992). *Sliding modes in control optimization*, Springer-Verlag, Berlin, Germany.

Yang, J. N., Li, Z., and Liu, S. C. (1992). "Stable controllers for instantaneous optimal control algorithm." *J. Engrg. Mech.*, ASCE, 118(8), 1612–1630.

Yang, J. N., Li, Z., and Wu, J. C. (1993). "Discontinuous nonlinear control of base-isolated building." *Proc. Int. Workshop on Structural Control*, G. W. Housner and S. F. Masri, eds., Univ. of Southern California, Los Angeles, Calif., 551–563.

Yang, J. N., Li, Z., Wu, J. C., and Hsu, I. R. (1994a). "Control of sliding-isolated buildings using dynamic linearization." *J. Engrg. Struct.*, 16(6), 437–444.

Yang, J. N., Wu, J. C., Agrawal, A. K., and Li, Z. (1994b). "Sliding mode control of seismic-excited linear and nonlinear civil engineering structures." *Technical Report NCEER-94-0017*, Nat. Ctr. for Earthquake Engrg. Res., Buffalo, N.Y.

Yang, J. N., Wu, J. C., Reinhorn, A. M., Riley, M., Schmitendorf, W. E., and Jabbari, F., (1994c). "Experimental verifications of H_∞ and sliding mode control for seismic-excited structures." *Proc., 1st World Conf. on Struct. Control*, Int. Assoc. for Struct. Control, Los Angeles, Calif., TP4-63–TP4-72.

Young, K. D., ed. (1993). *Variable structure control for robotics and aerospace applications*. Elsevier, New York, N.Y.

Zhou, F., and Fisher, D. G. (1992). "Continuous sliding mode control." *Int. J. Control*, 55, 313–327.